Materials Transactions, Vol. 53, No. 3 (2012) pp. 571 to 574

EXPRESS REGULAR ARTICLE

Characteristics of Thin-Film-Transistors Based on Zn–In–Sn–O Thin Films Prepared by Co-Sputtering System

K. J. Chen[1,2], F. Y. Hung[2,*], T. S. Lui[2], S. J. Chang[3] and T. Y. Liao[3]

[1]*The Instrument Center, National Cheng Kung University, Tainan 701, Taiwan, R. O. China*
[2]*Department of Materials Science and Engineering, Institute of Nanotechnology and Microsystems Engineering, Center for Micro/Nano Science and Engineering, National Cheng Kung University, Tainan 701, Taiwan, R. O. China*
[3]*Institute of Microelectronics & Department of Electrical Engineering, National Cheng Kung University, Tainan 701, Taiwan, R. O. China*

This study presents the growth of ZITO film by co-sputtering system. By adjusting the chemical composition and electrical properties of ZITO, an amorphous ZITO (a-ZITO) matrix with a semiconducting character was used to apply in active layer for thin-film transistors (TFTs) device. The proposed a-ZITO channel layer with SiN_x dielectric layer exhibited depletion mode operation. The device exhibited a subthreshold swing (*SS*) of 1.65 V/dec, a field-effect mobility (μ_{FE}) of 2.57 $cm^2 V^{-1} s^{-1}$, and an on/off current ratio (I_{on}/I_{off}) of 10^4. The small *SS* and an acceptable μ_{FE} were associated with a smaller roughness and stable composition of ZITO channel layer. [doi:10.2320/matertrans.M2011347]

(Received November 10, 2011; Accepted December 19, 2011; Published February 25, 2012)

Keywords: *zinc–indium–tin–oxygen (ZITO), co-sputtering, thin-film transistors (TFTs), depletion mode*

1. Introduction

Recently, the various quaternary materials have been extensively researched for requiring a better performance of optoelectronic devices, such as Zn–In–Sn–O (ZITO),[1,2] In–Ga–Zn–O (IGZO),[3] Cu–In–Ga–S (CIGS)[3] and Cu–Zn–Sn–Se (CZTSe).[4] Particularly, the ZITO material simultaneously possesses ZnO and ITO characteristics that can be applied in many fields of optoelectronics.[5–8] The present study uses multi-compound ZITO material and applies in channel layer of thin-film transistors (TFTs).

Many different ZnO-based TFTs became emerging devices and strongly expected to replace conventional silicon TFTs because of their good device performance, and potential for transparent and flexible active circuits.[9,10] However, the composition of ZnO-based crystallization is not stable enough that can affect the performance of TFTs. According to our previous report,[11] the additional indium and tin doping promoted a more stable equilibrium the ZITO matrix that can help the performance of the optoelectronics devices improvement.

The growth of the proposed ZITO film use the co-sputtering system and its properties for TFTs is adjusted by adjusting ZnO content in ZITO matrix and O^2 gas concentrations.[6] The structural and electrical of ZITO film was examined. The TFTs device use amorphous and semiconducting ZITO to serve as channel layer, and clarifies its electrical characteristics.

2. Experimental Procedures

Zn–In–Sn–O (ZITO) thin films were deposited onto a silica glass substrate by ZnO target (99.99%, Φ2″) and ITO target (99.99%, Φ2″) using co-sputtering system (ULVAC, Model ACS-4000-C3). The distance between target and substrate was maintained at 150 mm, and this depositing process was performed under a pressure of 1.9×10^{-1} Pa. The RF power supplied to ZnO target was fixed at 80 W while the DC power supplied to ITO target was varied from 10 to 40 W, respectively. Due to the In_2O_3 phases mainly dominated the ITO structure; therefore the tin atomic concentration was out of consideration. As a result, the ZITO films were referred to the ratio of zinc atomic concentration to total atomic concentration of zinc and indium [Zn/(Zn + In) at%]. To achieve the semiconductor characteristic ZITO film, an amorphous ZITO (a-ZITO) was selected to adjust under the different oxygen partial pressures.

The compositions of ZITO films were measured using an attached energy dispersive X-ray (EDX) spectroscope of high-resolution thermal field emission scanning electron microscope (FE-SEM, JEOL/JSM-7001). The crystalline phase of ZITO films was examined by multipurpose X-ray thin film diffraction (XRD, Rigaku). The optical transmittance and the current–voltage (*I–V*) characteristics were measured by an UV–visible spectroscopy and a Semiconductor Parameter Analyzer (Agilent/4155-B), respectively.

3. Results and Discussions

3.1 Structural and electrical characteristics of ZITO film

Figure 1(a) shows X-ray diffraction patterns of ZITO films with different zinc atomic concentration ratio (58–89 at%). In the 89 at% Zn sample, the film presented a polycrystalline structure and ZnO phase (002) dominated the ZITO structure. As the Zn atomic concentration ratio decreased (76 at%), the intensity of In_2O_3 related diffraction peak increased and the $Zn_2In_2O_5$ phase appeared. Following, the polycrystalline structure was transformed into an amorphous-like structure when the Zn atomic concentration ratio reached 69%. This result may associate with the formation of $Zn_3In_2O_6$ structures resulted in the transformation of the ZITO crystallization. Notably, the intensity of this amorphous-like structure was not strong enough to reveal its crystallization

*Corresponding author, E-mail: fyhung@mail.ncku.edu.tw

Table 1 Resistivity and the average transmittance in visible range of ZITO film with various oxygen gas concentration.

	Conductor	Semiconductor				
$O_2/(O_2 + Ar)$ (%)	0	2.0	3.8	5.7	7.4	8.2
Resistivity (Ω*cm)	9.2×10^{-4}	2.8×10^{4}	6.1×10^{5}	7.0×10^{5}	1.0×10^{6}	3.9×10^{6}
Transmittance (%) 390–800 nm	89.7	80.5	81.0	81.5	80.4	81.0

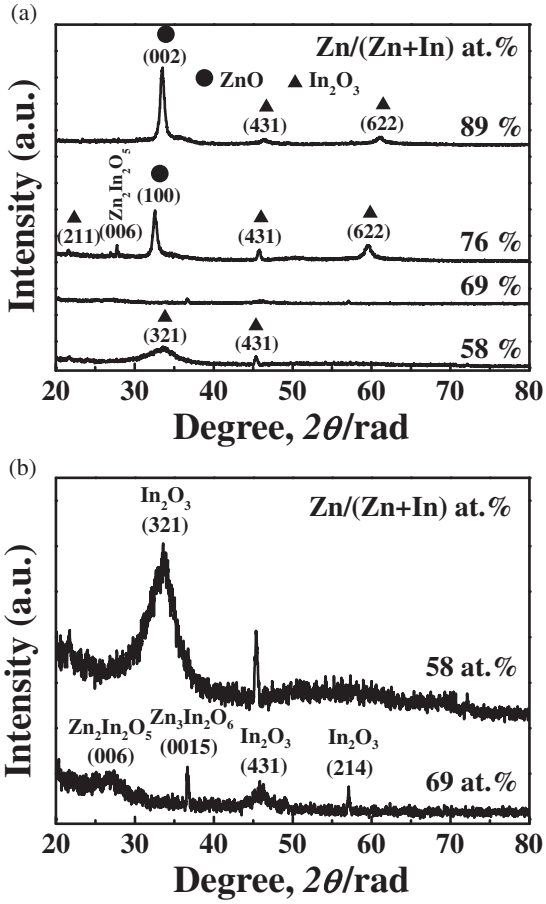

Fig. 1 X-ray diffraction patterns of ZITO films deposited with different zinc atomic content ratios. (a) 58–89% and (b) magnified pattern of 69% film.

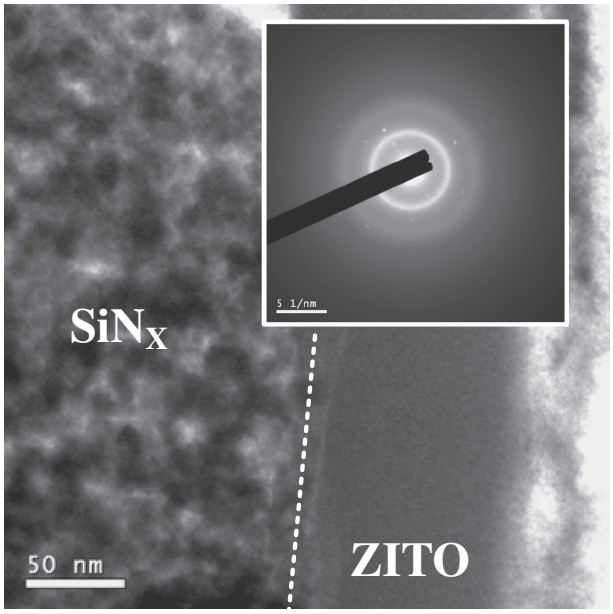

Fig. 2 Low magnification image and select area electron diffraction pattern of ZITO film (69% of Zn atomic content ratio) with oxygen concentration of 7.4%.

phase. Therefore, the XRD pattern of 69 at% Zn sample was singly appeared in Fig. 1(b). In fact, the crystallization of this ZITO film (69 at%) was dominated by In_2O_3 phase, $Zn_2In_2O_5$ phase and $Zn_3In_2O_6$ phase. This ZITO crystallization was similar to an amorphous structure of previous literature that may be applied in transistors.[12)]

Although this ZITO crystallization possessed an amorphous characteristic, but its electrical properties was not suitable for active layer of transistors (Table 1). To achieve the semiconductor characteristic, the ZITO film contained 69 at% of Zn (RF power: 80 W, DC power: 30 W) was selected to adjust the resistivity under the different oxygen concentrations. Table 1 presents the resistivity and optical transmittance in visible range (390–800 nm) of ZITO film (69 at% Zn) under the different oxygen concentrations (0–8.2%). As oxygen gas injected (O_2 concentration: 2.0%), the film resistivity rapidly increased from 9.2×10^{-4} to 2.8×10^{4} Ω*cm. This result indicated that the existence of more oxygen interstitials resulted in the increment of electron-trapping centers.[13,14)] With increasing the oxygen gas concentration the film resistivity gradually raised and then tended towards stability. As the oxygen gas concentration was more than 3.8%, the ZITO film possessed a semiconductor characteristic ($>6.1 \times 10^{5}$ Ω*cm) that could be applied in active layer of TFT devices.[15)] Additionally, the optical transmittance of ZITO film as a function of different oxygen gas concentration was shown in Table 1. It clearly showed that the average transmittance in the visible range (390–800 nm) of film reduced when the atmosphere changed from pure argon to an oxygen concentration of 2%. This result implied that the film roughness rose resulted in the increment of optical scattering.[16)] With increasing the oxygen concentration (2.0 to 8.2%), the average transmittances in the visible range of all films were approximately 81% which implied that the influence of oxygen concentration on optical transmittance of ZITO films was not obvious.

3.2 Fabrication of Zn–In–Sn–O thin film transistors (TFTs)

Further check the crystallization characteristic of ZITO active layer, the bright filed image and select area electron diffraction (SAED) pattern were carried out by a high resolution thermal filed emission transmission electron

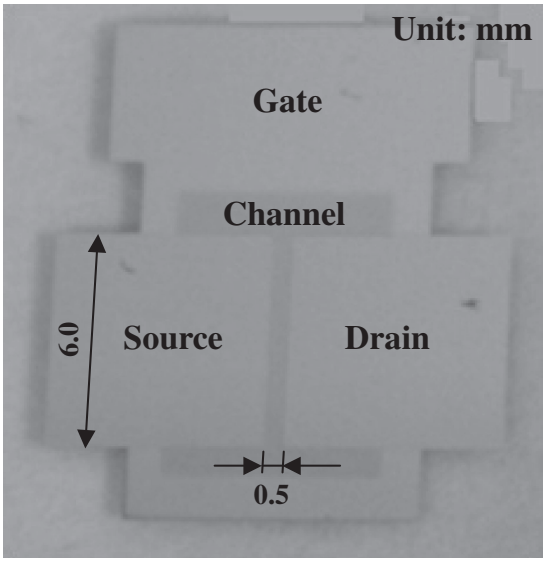

Fig. 3 The photograph of ZITO thin-film transistor.

microscopy (TEM), as shown in Fig. 2. This image shows a SiN_x dielectric layer and an 80 nm ZITO layer [$O_2/(O_2 + Ar) = 7.4\%$], and has no cracks in the interface. The SAED pattern confirmed that the ZITO layer was an amorphous crystallization (inset of Fig. 2). According to above results (Table 1 and Fig. 2), the ZITO film under an atmosphere contained 7.4% oxygen was suitable for candidate of TFTs active layer.

The 100 nm aluminum (Al) and 100 nm gold (Au) with shadow mask was deposited by a thermal evaporator to serve as the electrode for the bottom gate and top contact (source/drain electrode), respectively. 200 nm SiN_x was deposited by plasma enhanced chemical vapor deposition (PECVD, Oxford Plasmalab System 100). Then, a-ZITO channel layer [$O_2/(O_2 + Ar) = 7.4\%$] of 50 nm was grown upon SiN_x dielectric layer by the co-sputtering system. The channel length and width was 0.5 and 6.0 mm, respectively. The photograph of typical bottom gate ZITO TFT device structure was shown in Fig. 3.

The electrical properties of ZITO TFTs were performed within the dark box using a semiconductor parameter analyzer (Agilent/4155-B). Figure 4(a) shows drain current–drain voltage (I_D–V_{DS}) output characteristics of ZITO TFTs. The I_D–V_D curves exhibited typical transistor characteristics. The channel conductivity increased with increasing the positive gate bias which indicated that the ZITO TFTs device was attributed to n-channel device.[17] Figure 4(b) shows transfer characteristics of the drain current (I_D) as a function of gate voltage (V_G) under the drain voltage (V_D) of 2 V for ZITO TFTs. This device clearly showed a drain current on-to-off ratio (I_{on}/I_{off}) of approximately 10^4. By fitting the data of the square root of I_D–V_G in the saturation, the threshold voltage (V_T) was estimated to be about −4.4 V which meant that this TFTs device operated in depletion mode. The filed-effect mobility (μ_{FE}) can be calculated in linear region by the following equation,[18]

$$\mu_{FE} = \frac{L}{C_{ox} W V_D} g_m \quad (1)$$

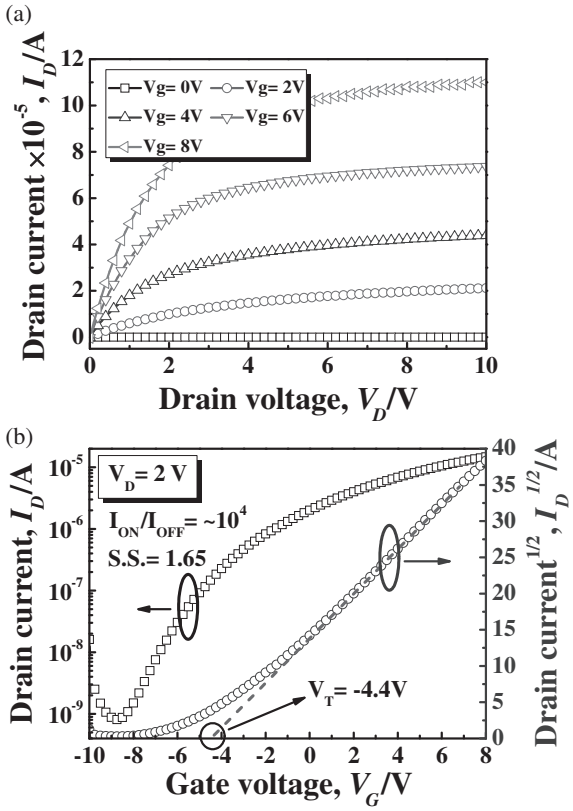

Fig. 4 (a) I_D–V_{DS} output characteristics of ZITO TFT device (b) $\sqrt{I_D}$–V_{GS} transfer characteristics under drain voltage of 2 V for ZITO TFT.

Table 2 Comparison of thin-film transistors with ZITO and ZnO active layer.

	ZITO (present work)	ZnO[20]	ZnO[21]
μ_{FE} ($cm^2 V^{-1} s^{-1}$)	2.57	1.70	1.13
V_T (V)	−4.4	2.5	0.8
SS (V/dec)	1.65	3.82	1.65
I_{on}/I_{off}	10^4	10^5	10^6

where C_{ox} is gate oxide capacitance per unit area; L and W are channel length and width, respectively; and $g_m((\frac{\partial I_D}{\partial V_D})_{V_G=const.})$ is the transconductance. This device exhibited an acceptable μ_{FE} of 2.57 $cm^2 V^{-1} s^{-1}$ that was satisfactory for liquid crystal display (LCD) pixel transistors.[19] The subthreshold swing (*SS*) is also a particular parameter to display the control ability of device turn-on and off, and it can be defined as:

$$SS = \frac{dV_G}{d(log I_D)} \quad (2)$$

From the transfer characteristics shown in Fig. 4(b), the *SS* was determined to be 1.65 V/dec.

Table 2 shows a comparison of the major characteristics of TFTs with ZITO and ZnO channel materials. Comparing with ZnO-based TFTs, the present TFTs devices has a higher mobility. This result associated with the smaller roughness of the interfaces between the SiN_x dielectric layer and ZITO channel layer.[19,20] Additionally, a few amount of In_2O_3 and SnO_2 crystal integrated with ZnO that can promote the stability of ZITO crystallization.

4. Conclusions

This work uses the co-sputtering system to grow the multi-compound ZITO, and control the ZnO and O^2 gas concentration to adjust the crystallization and electrical characteristics. The transformation of the ZITO matrix from polycrystalline to amorphous associated with the formation of $Zn_3In_2O_6$ structures. As the zinc atomic content ratio of in ZITO matrix got to be 69% and O^2 gas partial pressure got to be over 2%, the ZITO matrix possessed amorphous and semiconducting properties that can applied in channel layer for TFTs device. The present ZITO TFTs exhibited a depletion mode operation with μ_{FE} of $2.57\,cm^2\,V^{-1}\,s^{-1}$, a small *SS* of 1.65 V/dec, and an average I_{on}/I_{off} of 10^4. A smaller *SS* value and acceptable μ_{FE} attributed to a smaller surface roughness and stable equilibrium the ZITO channel layer. These results reveal that ZITO is a promising active layer material for TFTs.

Acknowledgements

The authors are grateful to The Instrument Center of National Cheng Kung University, the Center for Micro/Nano Science and Technology (D100-2700) for the financial support under grant numbers NSC 100-2221-E-006-094 and NSC 100-2221-E-006-092.

REFERENCES

1) M. G. Kim, H. S. Kim, Y. G. Ha, J. Q. He, M. G. Kanatzidis, A. Facchetti and T. J. Marks: J. Am. Chem. Soc. **132** (2010) 10352–10364.
2) C. A. Hoel, T. O. Mason, J. F. Gaillard and K. R. Poeppelmeier: Chem. Mat. **22** (2010) 3569–3579.
3) C. J. Chiu, S. P. Chang and S. J. Chang: IEEE Electron Device Lett. **31** (2010) 1245–1247.
4) K. Maeda, K. Tanaka, Y. Fukui and H. Uchiki: Sol. Energy Mater. Sol. Cells **95** (2011) 2855–2860.
5) J. Liu, D. B. Buchholz, R. P. H. Chang, A. Facchetti and T. J. Marks: Adv. Mater. **22** (2010) 2333–2337.
6) K. J. Chen, F. Y. Hung, S. J. Chang, S. P. Chang, Y. C. Mai and Z. S. Hu: J. Alloy. Compd. **509** (2011) 3667–3671.
7) G. S. Heo, Y. Matsumoto, I. G. Gim, H. K. Lee, J. W. Park and T. W. Kim: Solid State Commun. **150** (2010) 223–226.
8) E. Budianu, R. Muller, M. Purica, L. Eftime, R. Skarvelakis and G. Kiriakidis: Thin Solid Films **518** (2009) 1057–1059.
9) C. Y. Lee, M. Y. Lin, W. H. Wu, J. Y. Wang, Y. Chou, W. F. Su, Y. F. Chen and C. F. Lin: Semicond. Sci. Technol. **25** (2010) 105008.
10) D. C. Paine, B. Yaglioglu, Z. Beiley and S. Lee: Thin Solid Films **516** (2008) 5894–5898.
11) K. J. Chen, F. Y. Hung, S. J. Chang, S. J. Young, Z. S. Hu and S. P. Chang: J. Sol-Gel Sci. Technol. **54** (2010) 347–354.
12) G. S. Heo, Y. Matsumoto, I. G. Gim, J. W. Park, G. Y. Kim and T. W. Kim: Jpn. J. Appl. Phys. **49** (2010) 035801.
13) K. C. Liu, J. R. Tsai, C. S. Li, P. H. Chien, J. N. Chen and W. S. Feng: Jpn. J. Appl. Phys. **49** (2010) 04DF21.
14) P. K. Shin, Y. Aya, T. Ikegami and K. Ebihara: Thin Solid Films **516** (2008) 3767–3771.
15) Y. K. Moon, S. Lee, D. H. Kim, D. H. Lee, C. O. Jeong and J. W. Park: Jpn. J. Appl. Phys. **48** (2009) 031301.
16) B. L. Zhu, S. J. Zhu, X. Z. Zhao, F. H. Su, G. H. Li, X. G. Wu and J. Wu: Phys. Status Solidi A **208** (2011) 843–850.
17) M. S. Grover, P. A. Hersh, H. Q. Chiang, E. S. Kettenring, J. F. Wager and D. A. Keszler: J. Phys. D **40** (2007) 1335–1338.
18) D. K. Schroder: *Semiconductor Material and Device Characterization*, 2nd ed., (John Wiley & Sons, New York, 1998).
19) N. C. Su, S. J. Wang, C. C. Huang, Y. H. Chen, H. Y. Huang, C. K. Chiang, C. H. Wu and A. Chin: Jpn. J. Appl. Phys. **49** (2010) 04DA12.
20) T. T. Trinh, V. D. Dguyen, K. Ryu, K. Jang, W. Lee, S. Baek, J. Raja and J. Yi: Semicond. Sci. Technol. **26** (2011) 085012.
21) S. H. K. Park, C. S. Hwang, H. Y. Jeong, H. Y. Chu and K. I. Cho: Electrochem. Solid-State Lett. **11** (2008) H10.